

Flat-tipped Indentation Fracture Mechanics

Xiaozhi Hu^{1*} and Yujun Xie^{2*},

¹ School of Mechanical and Chemical Engineering, University of Western Australia, Perth, WA 6009, Australia

² Department of Mechanical Engineering, Liaoning Shihua University, Fushun, 113001, P. R. China

* Corresponding author: xiao.zhi.hu@uwa.edu.au, yjxie@lnpu.edu.cn

Abstract A singular stress field exists in an elastic substrate around the contact edge with a rigid flat-tipped indenter. This surface-contact-induced singular stress field can also be described by the stress intensity factor concept, if the indentation stress intensity factor K_{ind} is introduced for indentation cracking analysis. The K_{ind} -controlled singular stress field is almost identical to that of the Mode-I tensile singular stress field around the crack tip, except the negative sign due to the compressive nature of surface contact loading.

This study presents an energy-based fracture mechanics analysis for the indentation stress intensity factor (ISIF) K_{ind} and the indentation-induced boundary cracking within the K_{ind} -dominant region around the contact edge. It is found that the critical indentation stress intensity factor exists, and the relation between the indentation fracture toughness K_{IC-ind} and the common Mode-I fracture toughness K_{IC} is established analytically, showing $K_{IC-ind} = 2.5K_{IC}$. The indentation-cracking angle at the contact edge is also determined.

The fracture mechanics model on surface contact cracking induced by a flat-tipped indenter provides a useful alternative for measuring the fracture toughness K_{IC} , which can be useful for characterization of surface fracture properties of bulk elastic bodies and coating fracture properties of layered structures such as MEMS.

Keywords Indentation, Indentation fracture toughness, Contact mechanics, Surface cracking

1. Introduction

Frictional sliding induced surface damage in the form of micro-crack initiation can be the precursor for potentially much severe structural damage. Fracture mechanics modeling concerning this important structural integrity issue has been an interesting topic for years [1-3]. It is noted from the work [1,2,4,5] that a mixed-mode singular stress field exists in an incompressible substrate at the sliding contact edge of a rigid flat-ended indenter pressing down onto the substrate. This study will examine closely the process of micro-crack initiation on the contact surface, which is controlled by the singular stress field at the sharp corner of the flat-ended indenter, and the cracking angle.

The familiar singular stress fields are those associated with sharp cracks in elastic solids, through which the Mode-I fracture toughness K_{IC} at the critical loads can be determined from the common stress intensity factors. Although the singular stress field in an incompressible substrate at the sliding contact edge of a rigid flat-ended indenter is not due to the presence of a sharp crack tip, this contact-induced singular stress field does share some similar features with those of a crack-induced singular stress field, which implies the well-known concepts of linear elastic and elastic-plastic fracture mechanics such as the stress intensity factor K and the J -integral [6-11] can be adopted for modeling of the crack initiation from a crack-free surface under frictional sliding wear.

The significance of fracture mechanics modeling of contact crack initiation can be seen from fretting fatigue and other engineering applications such as rock fracture mechanisms in rock cutting. This study will present a new methodology based on the aforementioned singular stress field generated at the sliding contact edge of a rigid flat-ended indenter, which will connect the contact mechanics together with the fracture mechanics by using energy-based modeling.

2. The energy release rate for boundary cracking

This section describes the method we used to derive the strain energy release rate associated with sliding contact crack initiation from the crack-free boundary. The energy release rate related to a boundary movement has been investigated by Eshelby [6], Sih [7], Budiansky and Rice [8,9]. Consider a three-dimensional (3D) elastostatic boundary problem with material contained within the surface boundary $S+s$ (Fig. 1), where the portion s of the boundary is traction-free, and the external loading is imposed only on S . Without changing the boundary conditions on S , impose a continuously varying sequence of static solutions, related to the displacements u , given by a time-like parameter t . Details of the procedure can be consulted in references [9], and here, only the result of energy release rate per unit time, $\partial\Pi/\partial t$, is given, i.e.

$$\frac{\partial\Pi}{\partial t} = \int_s wv_i m_i ds, \quad (1)$$

where v_i denotes the ‘velocity’ of the points on s and m_i is the current outward normal to s . In the case of two-dimensional deformation fields as shown in Fig. 2, relevant to the present problem, the energy release rate remains of the same form as Eq. (1).

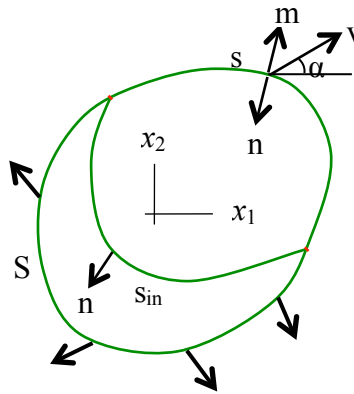


Figure 1. Two-dimensional deformation fields and integration path.

Let $v_i = e_i = \Delta/\Delta$, which corresponds to two components of unit boundary movement, so that $e_1 = \cos\alpha$, $e_2 = \sin\alpha$, where α is the angle between boundary movement Δ and x_1 . Let $n_i = -m_i$ be the unit tensor inward normal to boundary s , which means that the boundary s moves inward, and let all points on boundary s move in the same direction. Thus, the energy release rate for the boundary movement is given by

$$\bar{G} = -\frac{\partial\Pi}{\partial\Delta} = \int_s w e_i n_i ds = e_i J_i = J_1 \cos\alpha + J_2 \sin\alpha, \quad (2)$$

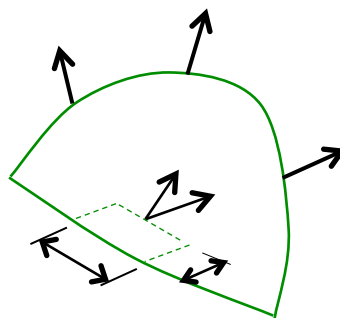


Figure 2. Boundary movement or cracking as $s \rightarrow 0$ the notch-like boundary becomes a crack.

and from the conservation law, J_i , proposed by Eshelby [6]

$$J_j = \int_s wn_j ds = \int_{s_{in}} (wn_j - T_i u_{i,j}) ds, \quad (3)$$

where s_{in} is any integration path within the area closed by boundary $S+s$, and $s_{in}+s$ form a closed integral loop.

From the geometrical point of view, boundary crack initiation, regardless whether it occurs at a crack tip, a notch corner or on a general crack-free boundary, can always be defined as a boundary movement in some direction, with the limit $s \rightarrow 0$ taken and the notch-like boundary becomes a crack, as shown in Fig. 2 and Fig. 3. Then, the energy release rate of boundary cracking can be defined as

$$G = (J_1)|_{s \rightarrow 0} \cos \alpha + (J_2)|_{s \rightarrow 0} \sin \alpha, \quad (4)$$

where $(J_1)|_{s \rightarrow 0}$ denotes the driving force of boundary cracking in direction x_1 when the limit taken exists, or the energy release rate with unit boundary movement s in direction x_1 ; $(J_2)|_{s \rightarrow 0}$ denotes the driving force in direction x_2 , or the energy release rate with unit boundary movement s in direction x_2 .

For a homogenous and isotropic substrate Griffith's criterion [9] states that the crack will extend when the critical value G_{max} is reached [10,11]

$$G_{max} = G_c. \quad (5)$$

For a standard cracked specimen subjected to Mode I loading, $G_{max} = J_1$ and G_c can be calibrated as

$$G_c = J_{IC} = K_{IC}^2(1 - \mu^2)/E, \quad (6)$$

where K_{IC} is the Mode-I fracture toughness.

3. Asymptotic stress field in sliding contact

3.1. Boundary Condition

A typical fretting contact problem of a rigid flat-ended indenter with half width a , sliding on a homogeneous, isotropic, elastic body in half plane is shown in Fig. 3. The Cartesian coordinates (x_1, x_2) , and the polar coordinates (r, θ) , both with the origin at the left edge of the indenter, are selected. Normal force P and tangential force Q act on the indenter and the following normal and shear tractions along interface have been solved in closed form [4],

$$p(x_1) = -\frac{P \sin \lambda \pi}{\pi} \left(2 - \frac{x_1}{a}\right)^{\lambda-1} \left(\frac{x_1}{a}\right)^{-\lambda} \quad (7)$$

and

$$q(x_1) = fp(x_1), \quad (8)$$

where f is the coefficient of friction; λ is determined by

$$\tan \lambda \pi = \frac{2(1-\mu)}{f(1-2\mu)}, \quad 0 < \lambda < 1 \quad (9)$$

and μ is Poisson's ratio of the substrate.

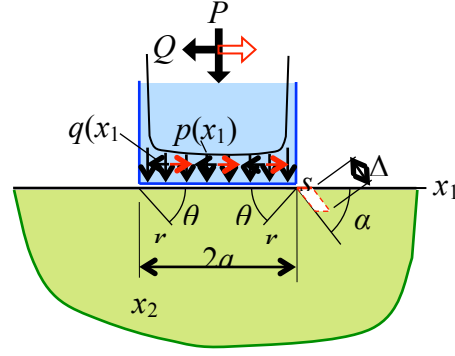


Figure 3. Indentation configuration, integral path $s \rightarrow 0$ and $\Delta \rightarrow 0$.

Eq. (7) shows that the stress state near the indenter corner may vary in the form

$$\sigma_{ij} = \begin{cases} 0(r^{\lambda-1}), & x_1 = 2a \\ 0(r^{-\lambda}), & x_1 = 0 \end{cases} \quad \text{as } r \rightarrow 0. \quad (10)$$

For special cases either with $\mu = 0.5$ or $f = 0$, Eq. (9) leads to $\lambda = 0.5$, showing the same order of stress singularity as that for a sharp crack tip.

For $\mu = 0.5$, the substrate becomes incompressible. The asymptotic stress boundary conditions of the substrate in the contact area next to the left and right corners then become

$$\sigma_{22}|_{\theta=0} = -\frac{P}{\pi\sqrt{2ar}} \quad (11)$$

and

$$\sigma_{21}|_{\theta=0} = \frac{fP}{\pi\sqrt{2ar}} \quad (12)$$

for the two cases of $\mu = 0.5$ and $f = 0$.

3.2. Singular stress fields due to the normal and tangential loads

The singular stress field at the sharp edge of the contact between a rigid flat-ended indenter and substrate is known from the asymptotic contact analyses of and Nadai [4]. Using the polar coordinates (r, θ) , Fig. 3, the stresses at the left corner can be found as follows due to the normal load:

$$\begin{pmatrix} \sigma_{rr}^I \\ \sigma_{\theta\theta}^I \\ \sigma_{r\theta}^I \end{pmatrix} = -\frac{K_{I-ind}}{\sqrt{2\pi r}} \begin{pmatrix} \cos \frac{\theta}{2} \left(1 + \sin^2 \frac{\theta}{2}\right) \\ \cos^3 \frac{\theta}{2} \\ \sin \frac{\theta}{2} \cos^2 \frac{\theta}{2} \end{pmatrix}. \quad (13)$$

This expression indicates that the stress state for indentation is a “negative” Mode I singular stress field for cracked solids, where

$$K_{I-ind} = \frac{P}{\sqrt{\pi a}}, \quad (14)$$

which defines actually an indentation stress intensity factor. The familiar Mode-I singular stress field is obtained by removing the negative sign and changing K_{I-ind} into K_I . Only difference between tensile mode-I stress field and indentation stress field is sign “-” in their equations.

Nadai [4] gave also the asymptotic stress field due to the tangential load as

$$\begin{pmatrix} \sigma_{rr}^{II} \\ \sigma_{\theta\theta}^{II} \\ \sigma_{r\theta}^{II} \end{pmatrix} = \frac{K_{II-ind}}{\sqrt{2\pi r}} \begin{pmatrix} \sin \frac{\theta}{2} \left(1 - 3 \sin^2 \frac{\theta}{2}\right) \\ -3 \sin \frac{\theta}{2} \cos^2 \frac{\theta}{2} \\ \cos \frac{\theta}{2} \left(1 - 3 \sin^2 \frac{\theta}{2}\right) \end{pmatrix}, \quad (15)$$

where

$$K_{II-ind} = fK_{I-ind} = \frac{fP}{\sqrt{\pi a}}. \quad (16)$$

Actually, Eq. (15) is identical to the classical Mode II singular stress fields when $K_{II-ind} = K_{II}$.

3.3. Characters of the stress fields

It is clear from the above discussion that the asymptotic stress field, $\sigma_{ij} = \sigma_{ij}^I + \sigma_{ij}^{II}$, induced by the sliding contact is a typical mixed-mode I-II singular stress field for incompressible substrates and friction free. This singular stress field is responsible for surface crack initiation on the crack-free surface of the substrate at the contact edge. This finding is significant as it shows that singularity and distribution of the stress field induced by surface contact of a flat-ended indenter are identical to those of a mixed-mode crack. As a result, the concepts of stress intensity factor and fracture toughness can now be introduced unambiguously into contact mechanics and associated contact damage. Therefore, Eqs. (14-17) represent an important advance by defining the indentation stress intensity factors, K_{I-ind} and K_{II-ind} , and the K_{ind} -dominant region at the contact edge. In other words, the fracture mechanics theory, such as the Griffith's criterion, is applicable in the case of the boundary fracture induced by the sliding contact.

4. Calculation methods on indentation stress intensity factor

4.1. Application of J_1 -integral in the indentation fracture

For a closed integration path $s_{abcdefa}$ as shown in Fig.4, following J_1 -integral can be gotten.

$$J_1 = \oint_{s_{abcdefa}} (wn_1 - T_i u_{i,1}) ds = 0. \quad (17)$$

If the path $s_{abcdefa}$ is divided into $s_{abcdefa} = s_{ab} + s_{bcd} + s_{de} + s_{afe}$, because of $n_1 = 0$ on surface of the substrate, $T_i = 0$ on the s_{ab} , $T_1 = 0$ and $u_{2,1} = 0$ on the s_{de} , we have

$$J_1 = \int_{s_{ab}} (wn_1 - T_i u_{i,1}) ds = 0 \quad (18)$$

and

$$J_1 = \int_{s_{de}} (wn_1 - T_i u_{i,1}) ds = 0. \quad (19)$$

Then substituting Eqs. (18) and (19) into Eq. (17), it follows that

$$J_1 = \int_{s_{abcdefa}} (wn_1 - T_i u_{i,1}) ds = - \int_{s_{afe}} (wn_1 - T_i u_{i,1}) ds + \int_{s_{bcd}} (wn_1 - T_i u_{i,1}) ds = 0. \quad (20)$$

It can then be rearranged to give

$$J_1 = \int_{s_{afe}} (wn_1 - T_i u_{i,1}) ds = \int_{s_{bcd}} (wn_1 - T_i u_{i,1}) ds, \quad (21)$$

which means that along any two paths, s_{afe} and s_{bcd} , starting from the any point on the left free boundary to any one on the contact boundary, the J_1 -integrals are identical. It shows theoretically

that this integral is path independent.

If the integration path s_{afe} is half of a circle and within the K_{ind} -dominant region, it is not difficult to get

$$J_1 = \int_{s_{afe}} (wn_1 - T_i u_{i,1}) ds = \frac{1-\mu^2}{2E} K_I^2 \quad (\text{plane strain}). \quad (22)$$

Then, Eq. (21) becomes

$$J_1 = \frac{1-\mu^2}{2E} K_I^2 = \int_{s_{bad}} (wn_1 - T_i u_{i,1}) ds \quad (23)$$

This equation is a key formula to construct a method to calculate the ISIFs induced by the indentation. Additionally, this method can be applied to the contact problems with the finite and infinite boundaries.

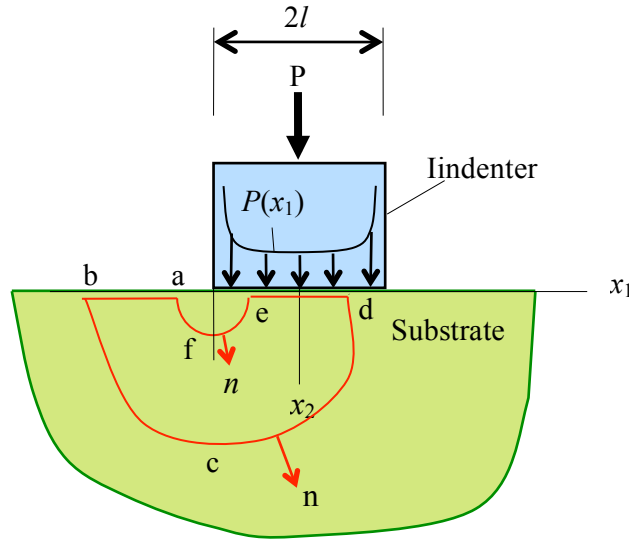


Figure 4. Integration path for Mode-I indentation.

4.2. Application of J_1 -integral in the indentation fracture for layered substrate

For the layered substrate, two closed integration paths as shown in Fig. 5 will be considered in present work. One is the part $s_1 = s_{mn} + s_{nedcbam}$ and the other $s_2 = s_{m'f'n'} + s_{n'm'}$. Additionally, as $n_1 = 0$, T_i and $u_{i,1}$ are continuous on the paths s_{mn} and $s_{n'm'}$, from conservation law, we have the following contour integrals.

$$J_1 = \int_{s_{mn}} T_i u_{i,1} ds + \int_{s_{nedcbam}} (wn_1 - T_i u_{i,1}) ds = 0 \quad \text{for the closed path } s_1, \quad (24)$$

$$J_1 = \int_{s_{m'f'n'}} T_i u_{i,1} ds + \int_{s_{n'm'}} (wn_1 - T_i u_{i,1}) ds = 0 \quad \text{for the closed } s_2. \quad (25)$$

$$\text{and } J_1 = \int_{s_{m'f'n'}} T_i u_{i,1} ds = - \int_{s_{mn}} T_i u_{i,1} ds \quad (26)$$

According to Eqs. (18), (19), (24)-(26), it can be found that

$$J_1 = \int_{s_{bcd}} (wn_1 - T_i u_{i,1}) ds = \int_{s_{afe}} (wn_1 - T_i u_{i,1}) ds, \quad (27)$$

which indicates that the integral is path independent for composite substrate similar to the Eq. (21).

If the integration path s_{bcd} is half circle and within the K_{ind} -dominant region, the following equation can be found.

$$J_1 = \frac{1-\mu_c^2}{2E_c} K_I^2 = \int_{s_{afe}} (wn_1 - T_i u_{i,1}) ds. \quad (28)$$

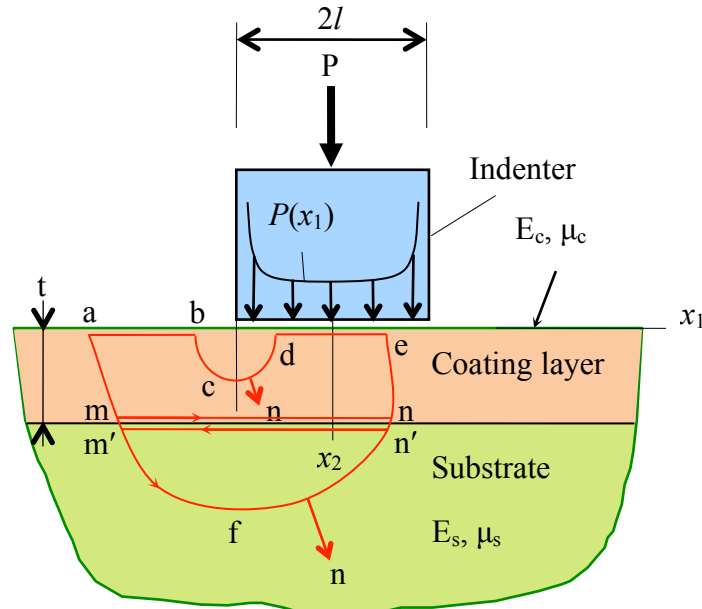


Figure 5. Integration path for the layered substrate for Mode-I indentation.

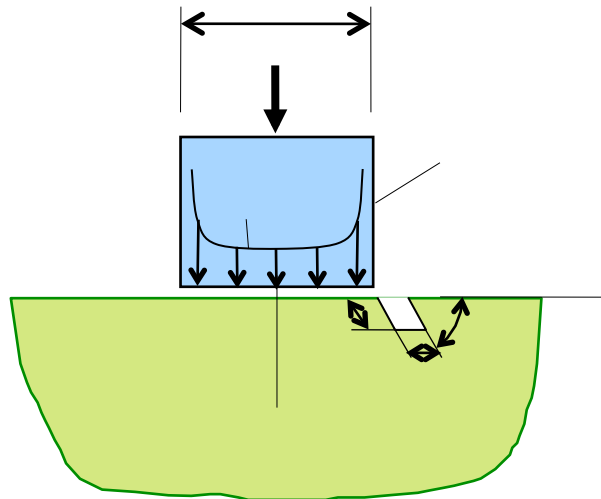


Figure 6. Boundary cracking for Mode-I indentation.

5. Boundary cracking in Mode-I indentation

In section 2, an expression describing the strain energy release rate of boundary cracking has been derived. It will be used to discuss the boundary cracking in the case of the complete sliding contact

in this section.

Let $s = s_{ob}$ in Eq. (3) as shown in Fig. 6 adjacent to the right corner of the indenter and s be within the K_{ind} -dominant region. Because $T_i = 0$ and $n_i = 0$ on the integration path s_{ob} , the energy-based driving force for boundary cracking in x_1 and x_2 directions in this case can be found in [12-16]

$$(J_1) \Big|_{s_{ob} \rightarrow 0} = \lim_{s_{ob} \rightarrow 0} \int_{s_{ob}} w n_1 ds = 0. \quad (29)$$

and

$$J_2 \Big|_{s \rightarrow 0} = \frac{(1 - \mu^2) K_{I-ind}^2}{2\pi E}, \text{ (plane strain)}. \quad (30)$$

From Eqs. (4), (29) and (30), the total energy release rate of boundary cracking induced by the sliding contact at any angle α can be found as

$$G = (J_1) \Big|_{s_{ob} \rightarrow 0} \cos \alpha + (J_2) \Big|_{s_{ob} \rightarrow 0} \sin \alpha = \frac{(1 - \mu^2) K_{I-ind}^2}{2\pi E} \sin \alpha. \quad (31)$$

Setting $\frac{dG}{d\alpha} = 0$, i.e., $\cos \alpha_c = 0$, we have

$$\alpha_c = \frac{\pi}{2}, \quad (32)$$

where α_c is the critical cracking angles, which is vertical to the contact boundary.

Cracking occurs when G reaches its critical or maximum value. The critical or maximum energy-based driving force for boundary cracking can then be solved from Eq. (31), i.e.

$$G_{\max} = \frac{(1 - \mu^2) K_{I-ind}^2}{2\pi E}. \quad (33)$$

From the Eqs. (5), and (33), the critical condition of substrate boundary cracking beneath the contact surface can be found as

$$G_{\max} = G_C = \frac{(1 - \mu^2) K_{IC-ind}^2}{2\pi E}. \quad (34)$$

for Mode-I indentation, where the K_{IC-ind} is the boundary fracture toughness for Mode-I indentation. Then, K-based fracture criterion for Mode-I indentation can be given by

$$K_{I-ind} = K_{IC-ind} \quad (35)$$

From Eqs. (34) and (6), it can be determined that

$$K_{IC-ind} = FK_{IC}, \quad (36)$$

where F is an enlarging factor, and is given by

$$F = \sqrt{2\pi} = 2.5066. \quad (37)$$

Therefore, Eq. (36) indicates that the common fracture toughness for a Mode-I tensile crack can also be determined by the indentation test method presented in this study. Recently, this indentation method has been successfully used to determine the fracture toughness of glass [16] and brittle polymers [17].

6. Conclusions

A fracture-based modelling for boundary cracking induced by indentation singular stress field has been investigated by using energy-based method. The concept of indentation stress intensity factor is introduced to describe the intensification of the indentation singular stress field. Typical calculation method on ISIFs has been given by using the partial J-integral. This study presents also an energy-based fracture mechanics analysis for the ISIF and the indentation-induced boundary

cracking within the K_{I-ind} -dominant region around the contact edge. It is found that the critical indentation stress intensity factor exists, and the relation between the indentation fracture toughness K_{IC-ind} and the common Mode-I fracture toughness K_{IC} is established analytically, showing $K_{IC-ind} = 2.5K_{IC}$. The indentation-cracking angle at the contact edge is also determined. The present fracture mechanics model on surface contact cracking induced by a flat-tipped indenter provides a useful alternative for measuring the fracture toughness K_{IC} , which can be useful for characterization of surface fracture properties of bulk elastic bodies and coating fracture properties of layered structures.

Acknowledgements

This work was supported by National Natural Science Foundation of China (Grant Nos. 50771052 and 50971068, 11272141), Gledden Senior Fellowship from the University of Western Australia and Natural Science Foundation of Liaoning (Grant Nos. LS2010100 and 20102129).

References

- [1]. A.E. Giannakopoulos, T.C. Lindley, S. Suresh, Aspects of connections and life-prediction methodology for fretting-fatigue. *Acta Mater*, 46 (1998) 2955-2968.
- [2]. A.E. Giannakopoulos, T.A. Venkatesh, T.C. Lindley, S. Suresh, The role of adhesion in contact fatigue. *Acta Mater*, 47 (1999) 4653-4664.
- [3]. B. Yang, S. Mall, On crack initiation mechanism in fretting fatigue. *ASME J Appl Mech*, 68 (2001) 76-80.
- [4]. A.I. Nadai, *Theory of flow and fracture of solids*. New York: McGraw-Hill, 1963.
- [5]. Y.J. Xie, D.A. Hills, Quasibrittle fracture beneath a flat bearing surface. *Eng Fract Mech*, 75 (2008) 1223–1230.
- [6]. J.D. Eshelby, The force on an elastic singularity. *Phil Trans Roy Soc London A* 244 (1951) 87-112.
- [7]. G.C. Sih, Inelastic behaviour of solids. In: Sih GC editor. *Dynamic aspects of crack aspects of crack propagation*, New York: Mc-Graw-Hill Book, Co, 1969, pp.607-639.
- [8]. J.R. Rice, A path-independent integral and the approximate analysis of strain concentrated by notches and cracks. *ASME J Appl Mech*, 35 (1968) 379-386.
- [9]. B. Budiansky, J.R. Rice, Conservation laws and energy-release rates. *ASME J Appl Mech* 40 (1973) 201-203.
- [10]. A.A. Griffith, The Phenomena of rupture and flow in solids. *Phil Trans Roy Soc London A* 221 (1921) 163-198.
- [11]. G.P. Cherepanov, *Mechanics of brittle fracture*. New York: McGraw-Hill International Book Co, 1979.
- [12]. Y.J. Xie, D.A. Hills, Quasibrittle fracture beneath a flat bearing surface. *Engineering Fracture Mechanics* 75 (2008) 1223–1230.
- [13]. Y.J. Xie, K.Y. Lee, X.Z. Hu, Y.M. Cai, Applications of conservation integral to indentation with a rigid punch. *Engineering Fracture Mechanics* 76 (2009) 949–957.
- [14]. Y.J. Xie, X.Z. Hu, X.H. Wang, J. Chen, K.Y. Lee, A theoretical note on mode-I crack branching and kinking. *Engineering Fracture Mechanics* 78 (2011) 919–929.
- [15]. Y.J. Xie, X.Z. Hu, X.H. Wang, Frictional contact induced crack initiation in incompressible substrate. *Engineering Fracture Mechanics*, 78 (2011) 2947–2956
- [16]. Y. J. Xie, X. Z. Hu, J. Chen and K.Y. Lee, Micro-indentation fracture from flat-ended cylindrical indenter. *Fatigue & Fracture of Engineering Materials & Structures*, 35 (2012) 45–55.
- [17]. X. Zhang, X.Z. Hu, Determination of fracture toughness of brittle polymers from contact crack induced by flat-tipped cylindrical indenter. *Polymer Testing*, 31 (2012) 765-769.